Investigations of Horizontal-Parallax-Only Optical Scanning Holography (HPO-OSH) through MATLAB Simulations

by

Enver Turan Akin

Thesis submitted to the Faculty of the Virginia Polytechnic Institute and State University in partial fulfillment of the requirements for the degree of

Master of Science
in
Electrical Engineering

Dr. Ting-Chung Poon, Chair
Dr. Scott F. Midkiff
Dr. A. Lynn Abbott

April 26, 2006
Blacksburg, Virginia

Keywords: Horizontal-paraxial-only optical scanning holography, digital holography

Investigations of Horizontal-Parallax-Only Optical Scanning Holography (HPO-OSH) through MATLAB Simulations

by

Enver Turan Akin

Dr. Ting-Chung Poon, Chair

Department of Electrical and Computer Engineering

(ABSTRACT)

The concept of generating horizontal-parallax-only (HPO) holograms by computer simulations is investigated. The simulations in this thesis are based on Optical Scanning Holography (OSH) aimed at acquiring HPO information electronically. The principles of OSH, a technique that allows the extraction of 3-D information by a 2-D optical scan of the object is first summarized. The HPO principles and simulation scenarios are then discussed. In order to illustrate the ideas, holograms were created and reconstructed using MATLAB simulations. The holograms are simulated by convolving the Fresnel zone plates (FZP) with the object. The simulations focus on generating HPO holograms using 1-D FZPs modeled as 1-D Gaussian chirp beams of varying waists. An optical reconstruction scheme by cylindrical lens was proposed and simulated. Three-dimensional imaging using HPO-holograms was also discussed. Several reconstruction scenarios were investigated by digitally convolving the complex HPO-hologram with the free space impulse response or the Gaussian chirp beam. Although many ideas of HPO-holography have been proposed and studied, to the best of our knowledge, this is the first proposed electronic technique to acquire HPO-holographic information. The simulations demonstrate that holographic information reduction techniques also help to alleviate the problems associated with the restricted field of view upon holographic reconstruction for 3-D display. The simulations show that horizontal-parallax-only holography is an excellent way to reduce holographic information. Suggested future work includes actual optical experimentation to verify the ideas presented in this thesis.

Acknowledgments

I wish to express my most sincere gratitude to my advisor, Professor Ting-Chung Poon. His unyielding support, patience and guidance have encouraged me throughout my program of study and I want to take this opportunity to thank him.
I would also like to thank Dr. A. Lynn Abbott and Dr. Scott F. Midkiff who most graciously advised me and served on my committee.

I would also like to thank my beloved wife and soul mate Susan for her endless encouragement, patience and ongoing assistance.

There are many people who have been incredibly supportive, but none more than my mother and father, Hatice and Muzafer Akin. To that end, I dedicate this thesis to their memory.

Table of Contents

List of Figures

Chapter 1: Introduction

Holograms inherently contain massive amounts of information that makes the transmission of holographic information a formidable challenge. The capacity of communication channels is limited. Reducing the information content of a hologram will help overcome this challenge. Horizontal-parallax-only (HPO) holography helps reduce the information content of holograms to facilitate the transmission. HPO-holograms show horizontal-parallax-only [1] information. Accordingly, the information reduction is implemented by sacrificing the vertical parallax. Since it is possible to display 3-D holographic images in real time, the transmission of holographic data and eventually the realization of a 3-D holographic television system may not be far off [2 ,3, 4].

This thesis focuses on generating HPO-holograms. Although many ideas of HPO-holography have been proposed and studied, to the best of our knowledge, this is the first proposed electronic technique to acquire HPO-holographic information. The images and holograms were created and reconstructed using MATLAB simulations. The simulations in this thesis are based on Optical Scanning Holography (OSH), a technique first suggested by Poon and Korpel in 1979 [5] and subsequently analyzed by Poon in 1985. Chapter 2 provides an introduction to OSH; a technique that allows the extraction of 3-D information by a 2-D optical scan of the object. In keeping with the holographic principle, OSH consists of recording or coding and reconstruction or decoding stages [6]. In the recording stage a 3-D object is 2-D scanned by a time -dependent Fresnel Zone Plate (TDFZP). The TDFZP is created by the interference of mutually coherent spherical and plane waves with

different temporal frequencies. The scattered light at the heterodyne frequency then extracts the amplitude and phase information of the scattered field [1]. As a result, in OSH, 2-D scanning performs correlation of the input object with a 2-D FZP [7]. Each point of the object is encoded as a 2-D FZP. Accordingly the recording represents the hologram of the object. During the scanning process, a photodetector collects the light transmitted through the object or scattered light if the object is diffusely reflecting and outputs a heterodyne scanned current that contains the TDFZP coded information of that object [8]. This current is then mixed down to become a demodulated signal. The demodulated signal is synchronized with the scans of the optical scanning system and fed to a 2-D display, which becomes the hologram of the scanned object. This can be stored in a computer or can be photographed as a transparency. Reconstruction of the hologram can be done optically or digitally. For example, if the transparency of the hologram is illuminated with coherent light, the diffraction pattern at a given distance will be representing the reconstructed hologram. The digital reconstruction could be achieved by convolving the stored hologram with the filter response at the desired plane at a given distance of interest [8].

The properties of imaging properties of optical heterodyne scanning have been examined by Poon and Indebetouw [9]. The principles of OSH have been studied by Poon, Wu, Shinoda and Suzuki [8], and Poon and Kim [7]. The OSH has been one of the major topics that was extensively examined by the Optical Image Processing Laboratory at Virginia Tech. Various applications of OSH have been examined by Kim's Masters thesis that focused on OSH for 3-D imaging of fluorescent objects in turbid media [10] and Schilling's doctoral dissertation on

Fluorescence Microscopy which provides a comprehensive reference for digital simulations of OSH [11]. Poon has examined OSH with a view to exploring the applications in holographic TV and laid the foundation for data reduction using horizontal-parallax-only (HPO) holography [3, 4]. A study by Lucerne demonstrates that the real-time display of holographic images is an attainable objective [2].

The HPO principles and simulation scenarios are discussed in Chapter 3. The simulations were performed using MATLAB. The object and the FZP were generated digitally. The simulations focus on generating HPO-holograms using 1-D FZPs modeled as 1-D Gaussian Chirp beams of varying waists. Secondly, an optical reconstruction scheme by cylindrical lens was proposed and simulated. Three-dimensional imaging using HPO-holograms was also discussed. Several reconstruction scenarios were investigated by digitally convolving the complex HPO-hologram with the free space impulse response or the Gaussian Chirp beam. Chapter 4 outlines the conclusions and suggested future work including actual optical experimentation to verify the ideas presented in this thesis.

Chapter 2: Introduction to Optical Scanning Holography (OSH)

2.1 Two-Pupil Optical Hetorodyne Scanning:

HPO-holography studied in this thesis is based on Optical Scanning Holography (OSH), a real-time holographic recording technique attributed to Poon and Korpel [5] that allows the acquisition of holographic information for a three-dimensional (3-D) object with a single 2-D optical scan of the object. The use of active optical heterodyne scanning has been examined extensively by Indebetouw and Poon [9]. OSH is executed by scanning an object with a temporally modulated Fresnel Zone Plate (TFZP).

As depicted in Figure 1, two laser beams of different temporal frequencies that carry the information of two different pupils ($p_1(x, y)$ and $p_2(x, y)$) are combined and used to scan an object in two dimensions by superimposing a spherical wave and a plane wave that originate from a single laser at a temporal frequency ω_0 [7, 11, 14]. Beam splitters BS along with BS_1 and mirrors M and M_1 form a Mach-Zehnder interferometer. The first beam from the collimated laser is at frequency ω_0 and is directed by a mirror to pass through a pupil ($p_1(x,y) =1$ for holographic applications). The frequency of the other path is offset by passing the beam through an acousto-optic frequency shifter (AOFS) operating in the Bragg regime (Figure 1) and the temporal frequency of this beam becomes $\omega_0 + \Omega$. This beam illuminates pupil $p_2(x, y)$. The two pupils are located at the front focal planes of lenses L_1 and L_2. The two lenses have the same focal length f. One of the collimated beams is focused by lens L_1 to form a point source on the 2-D scanning mirrors, which generates a spherical wave away

from the focused spot toward the 3-D object $I_0(x,y;z)$. The other collimated beam from L_2 forms a plane wave on the 3-D object, assuming $p_2(x, y) = \delta(x, y)$. The spherical wave and the plane wave are combined by beamsplitter BS_1 to form a time-dependent Fresnel zone plate (TDFZP). The two pupils are then combined by beam splitter BS_1 to focus the light onto the 2-D x-y scanning mirrors, which are located on the back focal plane of lenses L_1 and L_2. The combined optical scanning field is used to two-dimensionally raster scan over an object of amplitude distribution $I_0(x, y; z)$ at distance z away from the focal plane of the two lenses. The scattered light from the object is collected by Lens L3 onto the photodetector which gives a heterodyne current $i_\Omega(x, y)$ at frequency Ω as an output. The heterodyne current contains holographic information of the object being scanned.

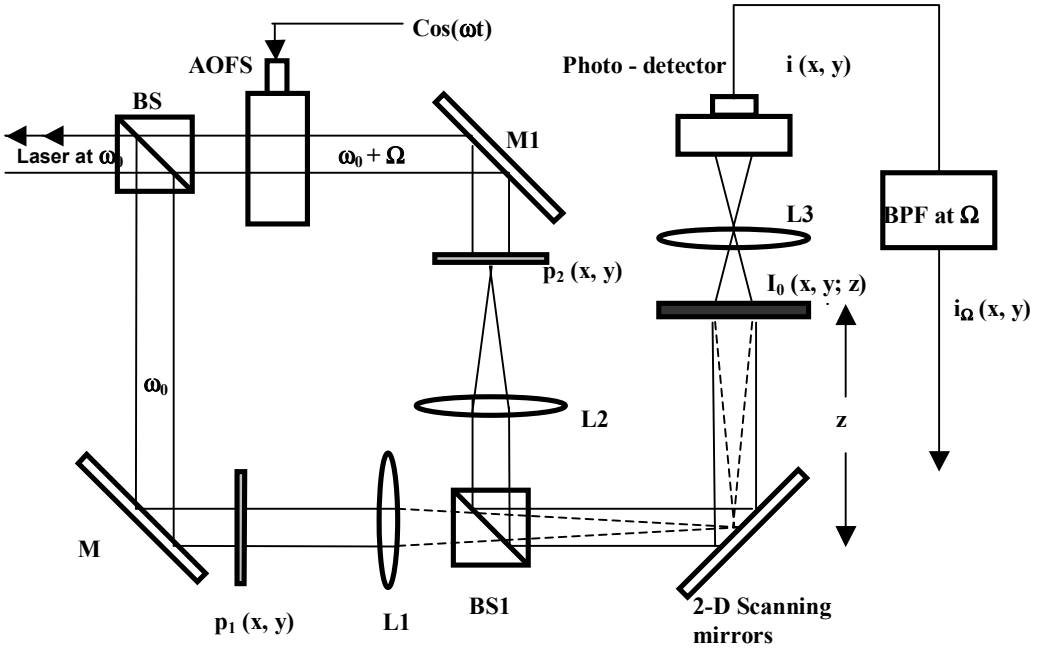

Figure 1 – Optical scanning holography setup - BPF denotes band pass filter

As depicted in Figure 2, when $i_\Omega(x, y)$ is mixed electronically with a sine and a cosine wave, the resultant outputs are denoted as follows:

$$i_c(x, y; z) = \mathrm{Re}[\mathcal{F}^{-1}\{\mathcal{F}\{|I_0|^2\}\mathrm{OTF}_\Omega\}]$$

$$= \mathrm{Re}[|I_0(x, y; z)|^2 \otimes h_\Omega(x, y; z)] \qquad \text{(Equation 1)}$$

$$i_s(x, y; z) = \mathrm{Im}[\mathcal{F}^{-1}\{\mathcal{F}\{|I_0|^2\}\mathrm{OTF}_\Omega\}]$$

$$= \mathrm{Im}[|I_0(x, y; z)|^2 \otimes h_\Omega(x, y; z)] \qquad \text{(Equation 2)}$$

where symbol $\otimes$ denotes a convolution operation. Symbols $\mathcal{F}$ and $\mathcal{F}^{-1}$ denote the Fourier and inverse Fourier transform operations respectively,

$h_\Omega(x, y; z) = \mathcal{F}^{-1}\{\mathrm{OTF}_\Omega\}$ is the point spread function (PSF) of the optical heterodyne scanning system. Poon and Kim have studied the derivation of the formulas used in this Chapter [7, 12]. OTF_Ω is the optical transfer function (OTF) of the system defined as [6]

$\mathrm{OTF}_\Omega(k_x, k_y; z) =$

$$\exp[j(z/2k_0)(k_x^2 + k_y^2)] \int\int p_1^*(x', y')p_2(x' + (f/k_0)k_x, y' + (f/k_0)k_y)$$

$$\exp[j(z/f)(x'k_x^2 + y'k_y^2)]dx'dy', \qquad \text{(Equation 3)}$$

where k_0 is the wave number of light and z is the distance from the focused spot on the 2-D scanning mirrors to the 3-D object as shown in Figure 1. The spatial frequencies corresponding to the coordinates x and y are denoted by k_x and k_y, respectively.

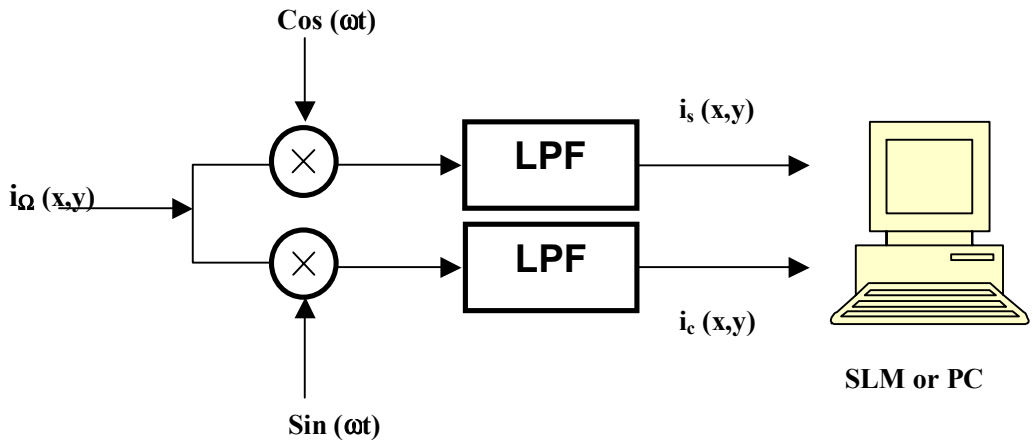

Figure 2 – i_Ω (x, y) mixed electronically with sine and cosine wave - LBF denotes low pass filter

In Equations (1, 2), we assume that the input object $|I_0(x, y; z)|^2$ is an infinitely thin 2-D object located a distance *z* away from the focus of the spherical wave, which is on the 2-D scanning mirrors as shown in Figure 1. In order to make these equations applicable to 3-D objects, we integrate them over the depth z of the 3-D object and obtain the following:

$$i_c(x, y) = \mathrm{Re}\left[\int \mathcal{F}^{-1}\{\mathcal{F}\{|I_0(x, y; z)|^2\}\mathrm{OTF}_\Omega\}\right]dz$$

$$= \mathrm{Re}\left[\int |I_0(x, y; z)|^2 \otimes h_\Omega(x, y; z)dz\right] \qquad \text{(Equation 4)}$$

$$i_s(x, y) = \mathrm{Im}\left[\int \mathcal{F}^{-1}\{\mathcal{F}\{|I_0(x, y; z)|^2\}\mathrm{OTF}_\Omega\}\right]dz$$

$$= \mathrm{Im}\int |I_0(x, y; z)|^2 \otimes h_\Omega(x, y; z)\, dz \qquad \text{(Equation 5)}$$

Equations (4, 5) represent recorded information for the 3-D object, $|I_0(x, y; z)|^2$. However, these equations are two-dimensional as they represent the

scanned and the processed versions of the 3-D object. To construct the holograms, the two pupils $p_1(x, y) = 1$ and $p_2(x, y) = \delta(x, y)$ are used. This setup is depicted in Figure. 1. Accordingly, the OTF of the scanning system, in Equations 4 and 5, becomes

$$OTF_{\Omega}(k_x, k_y ; z) = \exp[-j(z/2\, k_0)\,(k_x^2 + k_y^2)]$$
$$= OTF_{osh}(k_x, k_y ; z). \qquad \text{(Equation 6)}$$

The subscript osh denotes the OTF is for optical scanning holography. In this case, one of the holograms H(x,y), using Equation (4), is represented by

$$H(x,y) = \mathrm{Re}[\int \mathfrak{F}^{-1}\{\mathfrak{F}\{|\, I_0(x, y; z)|^2\}\, OTF_{osh}(k_x, k_y ; z)\}]dz$$
$$= \mathrm{Re}[\int \mathfrak{F}^{-1}\{\mathfrak{F}\{|\, I_0(x, y; z)|^2\}\exp[-j(z/2k_0)(k_x^2 + k_y^2)]\}dz]. \qquad \text{(Equation 7)}$$

Similarly, another hologram is given by the above equation with the operation Re replaced by Im. Equation (7) shows that holographic recording in the frequency domain can be interpreted as the object's spectrum is being processed by the OTF defined by Equation (6) [13]. By writing Equation (7) in terms of convolution, we can show that Equation (7) becomes

$$H(x, y) = \mathrm{Re}\,[\int |I_0|^2 \otimes h^*(x, y; z)]\, dz, \qquad \text{(Equation 8)}$$

where $h(x, y; z) = j\,(k_0/2\pi z) \exp[-j\,(k_0/2\pi z)\,(x^2 + y^2)]$ is the free space impulse response. Clearly, Equation (8) can be rewritten in terms of the correlation operation:

$$H_{sin}(x,y) = \mathrm{Re}[\int h(x, y; z) \square\, |I_0|^2\, dz$$

$$= \int k_0/(2\pi z)\sin [k_0/2z\ (x^2 + y^2)] \otimes |I_0|^2\, dz, \qquad \text{(Equation 9)}$$

where $\otimes$ denotes correlation defined as

$f(x, y) \otimes g(x, y) = \iint f^*(x', y') \otimes g(x + x', y + y')dx'dy'$. As an example, by letting $|I_0|^2$ $= \delta(x - x_0, y - y_0, z - z_0)$, we have $H_{sin}(x,y) = k_0/(2\pi z_0)\ \sin[k_0/2z_0\ [(x - x_0)^2 + (y - y_0)^2)]$ which is the hologram of an offset delta function located at a distance z_0 away from the scanning mirror. In general, $H_{sin}(x, y)$ given by Equation (9), is the sine-Fresnel zone plate of the object $|I_0|^2$. In optical scanning holography the 3-D holographic recording can be considered conceptually as a 2-D transverse correlation between the real part of the free-space impulse response, $k_0/(2\pi z)\sin[(k_0/2z\ (x^2 + y^2)]$ and the 3-D object, $|I_0(x, y; z)|^2$. The resulting correlation is then integrated along the depth of the object to obtain the hologram [7]. By replacing the Re operator with Im operator in Equation (9), the cosine hologram is obtained.

$H_{cos}(x, y) = \text{Im} [\int h(x, y; z) \otimes |I_0|^2\, d$

$$= \int k_0/(2\pi z)\cos[k_0/2z\ (x^2 + y^2)] \otimes |I_0|^2\, dz, \qquad \text{(Equation 10)}$$

where $H_{cos}(x, y)$ is the cosine-hologram of the object $|I_0|^2$. The complex hologram H_c is represented by [16]

$H_c = H_{cos}(x, y) - jH_{sin}(x, y) \propto h(x, y; z_0) \otimes |I_0(x, y)|^2$ (Equation 11)

where $I_0(x, y)$ is a planar object, located z_0 away from the scanning mirror.

2.2 Digital Implementation of Complex Holograms:

In OSH, the sine and cosine holograms could be obtained optically by using the setup depicted in Figure 1 and Figure 2. The complex holograms could then be generated digitally according to Equation (11). In this thesis, OSH process is simulated by using MATLAB. In these simulations, the object $|I_0(x, y)|^2$ was created using Microsoft PowerPoint and Microsoft Paint Brush. The object was scaled to 256 by 256 pixel image. The scanning pattern OTF_{osh} is created in frequency domain using Equation (6). In spatial domain the complex hologram is produced by the 2-D correlation of the FZP intensity pattern, $h(x, y; z_0)$ and the object's intensity transmittance or reflectance, $|I_0(x, y)|^2$ as in Equation (11). Digitally, the complex hologram was implemented using convolution. The 2-D convolution of f(x, y) and h(x, y) is given by [15]

$$f(x, y)\otimes h(x, y) = \iint f(x', y')h(x - x', y - y')dx'dy'. \qquad \text{(Equation 12)}$$

Per convolution theorem the Fourier transform pairs are defined as

$$f(x, y)\otimes h(x , y) \leftrightarrow F(k_x, k_y)\, H(k_x, k_y). \qquad \text{(Equation 13)}$$

The convolution is implemented in the frequency domain using the following relationship:

$$f(x, y) \otimes h(x, y) = \mathcal{F}^{-1}\{F(k_x, k_y)\, H(k_x, k_y)\} \qquad \text{(Equation 14)}$$

Accordingly, $OTF_{osh}(k_x, k_y; z_0)$ was implemented in the frequency domain and was multiplied by the Fourier transform of the image, $|I_0(x, y)|^2$. As depicted in the equation below, the complex hologram H_c in spatial domain is represented by:

$$H_c = \mathcal{F}^{-1}\{OTF_{osh}(k_x, k_y; z_0)\, \mathcal{F}[|I_0(x, y)|^2]\}. \quad \text{(Equation 15)}$$

Specifically, Figure 3 depicts a digitally generated planar object that is four dots on a black background. Figure 4 represents the real part of a digitally generated impulse response for OSH recording at distance z. This is represented by

$$\text{Re}\,[\mathcal{F}^{-1}\{OTF_{osh}(k_x, k_y; z_0)\}]. \quad \text{(Equation 16)}$$

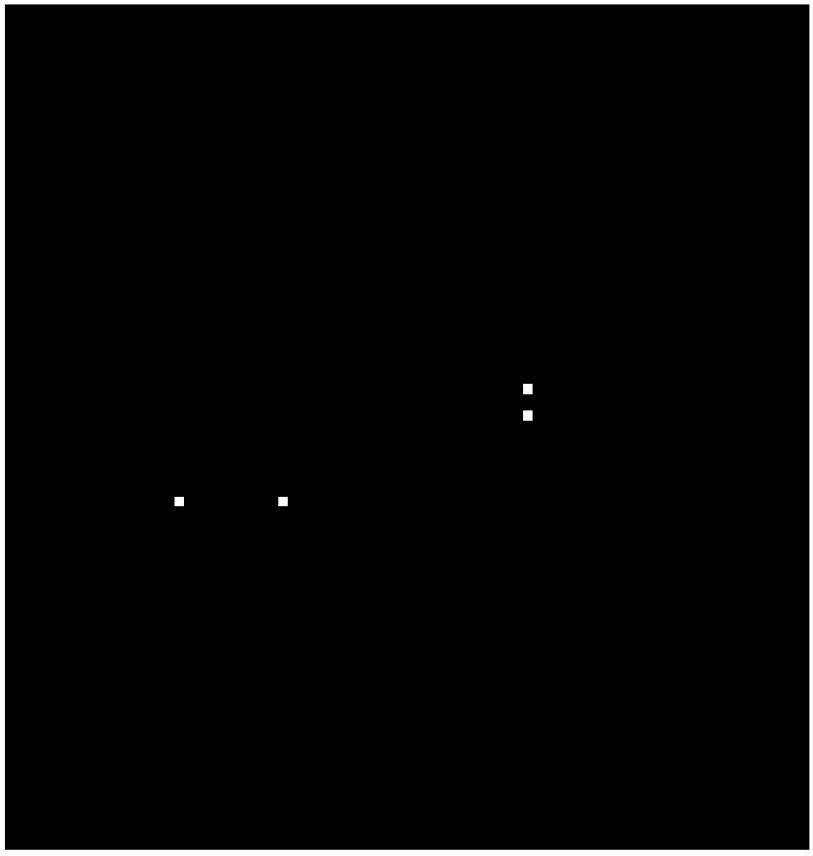

Figure 3 – Digitally generated planar object

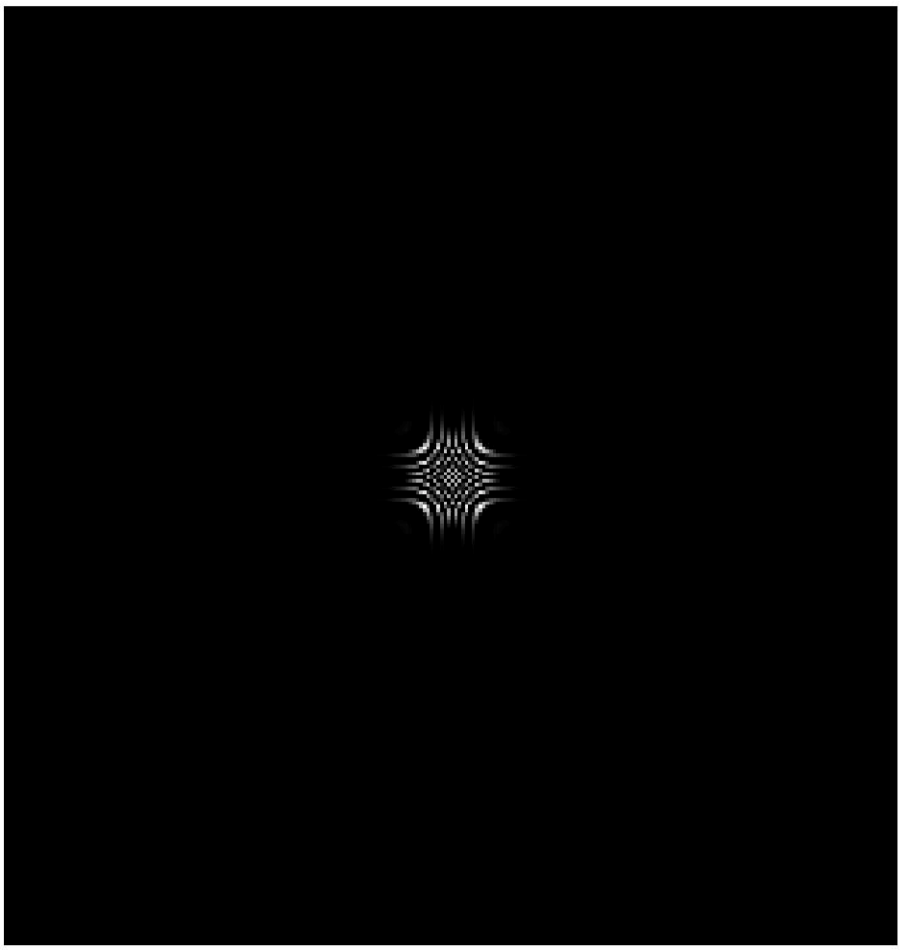

Figure 4 – Real part of the digitally generated impulse response

Figures 5 and 6 depict the sine and cosine holograms in accordance with Equations (9) and (10). Both the sine and cosine holograms are obtained simultaneously and given by replacing the Re [.] operation with Im [.].

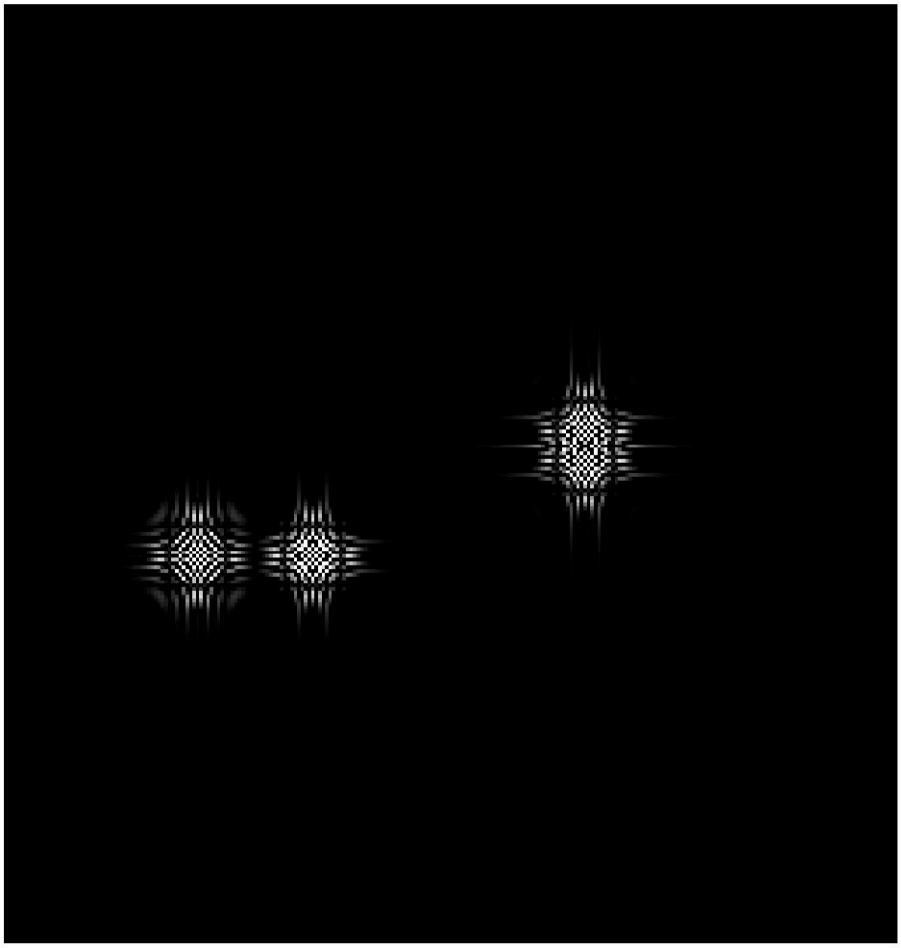

Figure 5 – Sine hologram

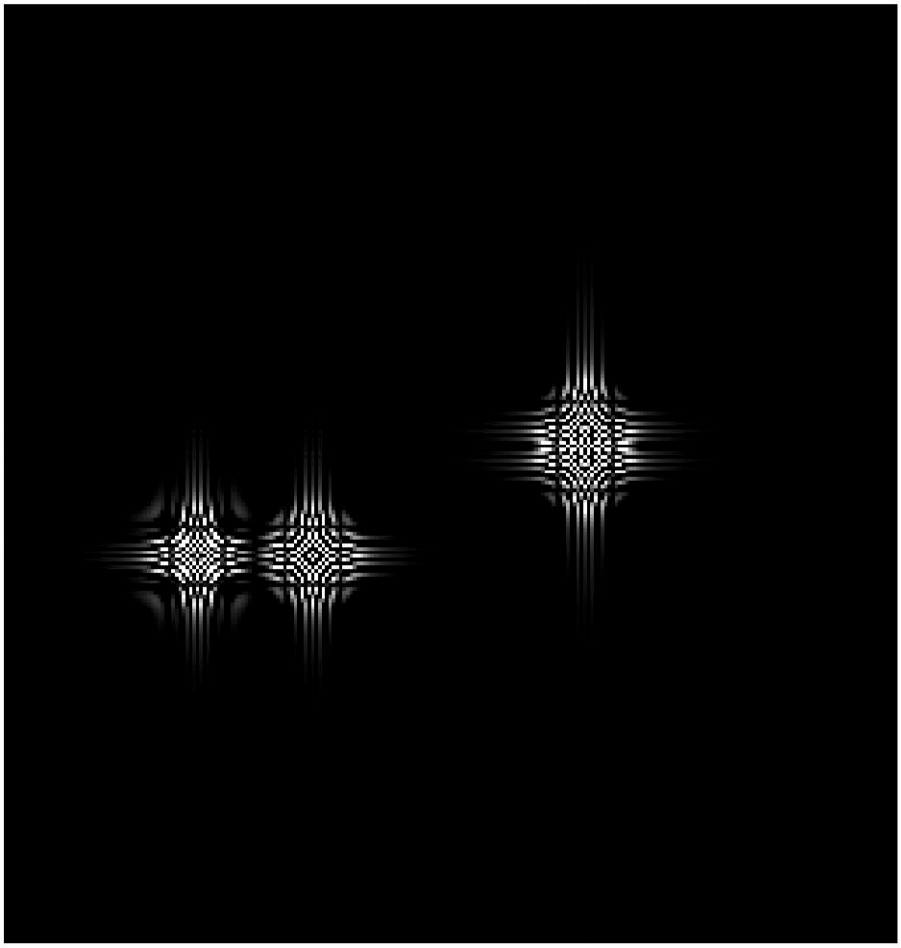

Figure 6 - Cosine hologram

2.3 Digital Reconstruction of Complex Holograms:

Holograms could be reconstructed by convolving the holograms with the free-space impulse response matched to the depth parameter z_0. Optical reconstruction is one way of doing this. Using this technique, the hologram is illuminated by a plane wave. Similarly, the hologram could be reconstructed digitally

by convolving the complex hologram (Equation 11), with the free space impulse response giving

$H_c(x, y) \otimes h(x, y; z)$ (Equation 17)

The reconstructed hologram is depicted in Figure 6. The dots are properly holographically focused along the x and y directions.

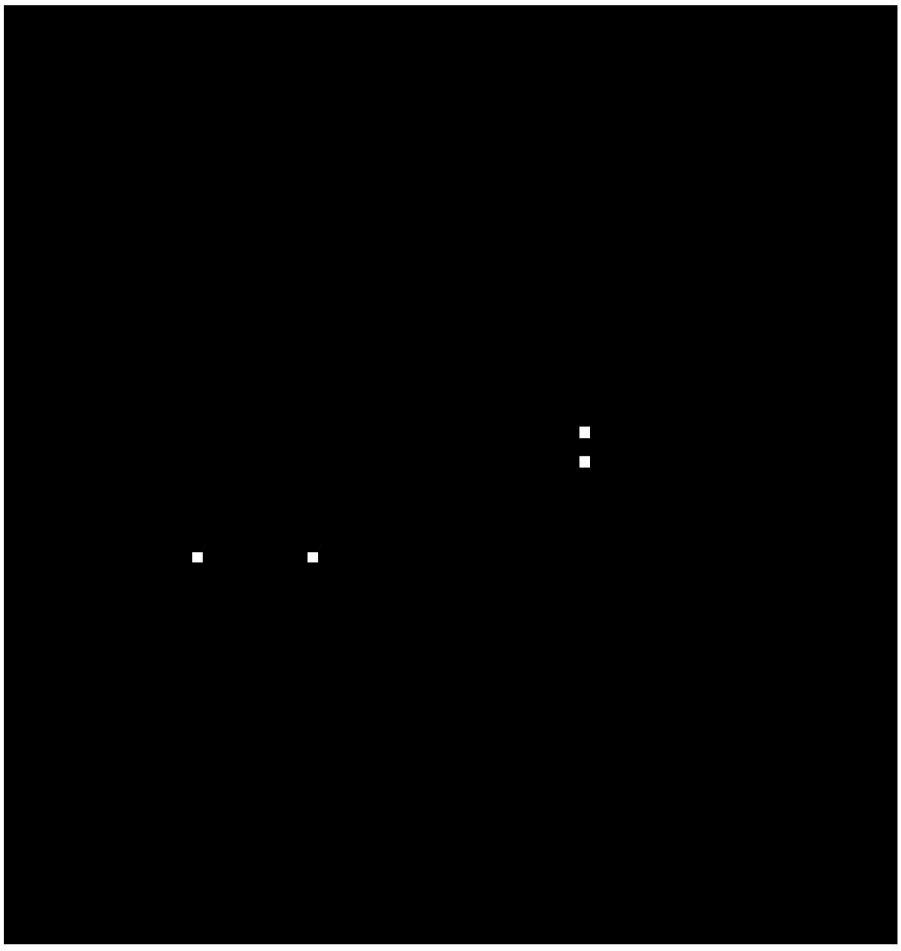

Figure 7 – Reconstructed hologram using 2-D scanning beam at z

2.4 OSH - Summary:

In summary, OSH is a real-time holographic recording technique in which holographic recording of 3-D objects is achieved by a single 2-D laser scanning. OSH is a hybrid technique that combines the advantages of optics and electronics OSH. The advantages of OSH are studied in detail by Poon, Wu, Shinoda and Suzuki [8]. Using OSH techniques, holographic recording and reconstruction could be achieved electronically. Electronic holography is an electronic processing technique that is used in the context of optical holography to bypass the use of films for recording. One salient advantage of OSH is the reduction of the channel bandwidth requirement by eliminating the twin image problem. In this context, the holographic information could be reduced by utilizing HPO-OSH. This technique and computer simulations are discussed in the next chapter.

Chapter 3: Horizontal-Parallax-Only Optical Scanning Holography (HPO-OSH)

HPO-OSH helps reduce the information content of holograms to facilitate the transmission. This is implemented by sacrificing the vertical parallax information. Accordingly, these holograms show horizontal-parallax-only information [1]. In this chapter, the recording and reconstruction of HPO-OSH digitally is discussed.

The applications information reduction using HPO-OSH has been studied by Poon who also proposed a real time holographic TV using OSH to acquire holographic information and using Spatial Light Modulators (SLM) for eventual coherent 3-D display [4]. In this context, HPO-OSH will reduce the data to a magnitude that will be manageable by present optical communication systems. Given a hologram of size d by d pixels for an on-axis point object hologram, the number of samples is $N = [d(2NA/\lambda)]^2$ where $\lambda/2NA$ is the resolvable element with $NA = \sin\theta$ where 2θ is the viewing angle. For a full parallax 20 mm by 20 mm on-axis hologram and a viewing angle of 60^0 with $\lambda = 0.6\mu m$, the required number of pixels is about 1.1 billion. Since we are used to observing our surroundings generally on a horizontal level, we are usually satisfied with only the horizontal parallax. HPO-OSH will reduce the required number of pixels significantly. For 512 vertical lines the number of required pixels become 512 by $d(2NA/\lambda)$ that is equal to approximately 17 million. Information reduction will also be significant for data transmission. Since the full parallax hologram requires about 1.1 billion pixels on the SLM, to update one frame with 8-bit resolution at 30 frames/s, a serial data rate of 1.1 billion samples/frame X 8 bits/sample X 30 frames/s =0.26 Tbit/s is required for full

parallax. With HPO-OSH the data rate becomes 4 billion bits/s, a rate that can be handled by modern optical communication systems.

The HPO-OSH is represented by stacked holo-lines that contain contributions only from points that lie on a single horizontal line of the object [1]. In OSH, the 3-D object is scanned by a 2-D TDFZP. Using this concept, HPO-OSH is realized by scanning the 2-D object by a 1-D TDFZP.

The 1-D scanning zone plate is implemented by masking the 2-D zone plate with a narrow Gaussian function represented by

$$s(x, y; z) = \exp[jk_0/(2z)\,(x^2 + y^2)]\exp\left[-(x/\omega_x)^2 - (y/\omega_y)^2\right] \qquad \text{(Equation 18)}$$

For a narrow line along y, we have $\omega_x >> \omega_y$. Every 1-D scan of the object will generate a single holo-line that contains holographic contributions solely from points that lie on a single horizontal line of the object. The horizontal-parallax-only holograms are obtained by stacking holo-lines vertically. As demonstrated in Chapter 2, scanning with a 2-D zone plate results in each scan line containing holographic information from the whole object yielding a full parallax hologram. Similar to Equation (11) for full-parallax holograms, the complex hologram in this scenario represented by

$$H_{c,HPO} = s(x, y; z_0) \otimes |I_0(x, y)|^2 \qquad \text{(Equation 19)}$$

$S(k_x, k_y)$, the Fourier transform of $s(x, y; z_0)$, was implemented in the frequency domain and was multiplied by the Fourier transform of the image $|I_0(x, y)|^2$. As depicted in the equation below the complex hologram H_c in spatial domain is represented by

$$H_{c,HPO} = \mathcal{F}^{-1}[S(k_x, k_y)\, \mathcal{F}\{|I_0(x, y)|^2\}] \qquad \text{(Equation 20)}$$

3.1 Simulations involving a single plane scanned with Gaussian beams with different widths:

The simulations were executed by using Gaussian scanning beams of different widths. The narrow beam was implemented by setting $\omega_X = 1000\omega_y$. Similarly, the wider beam was implemented by setting $\omega_X = 40\omega_y$ as in Equation (18). The wide and narrow Gaussian scanning beams are depicted in Figures 8 and 9 respectively.

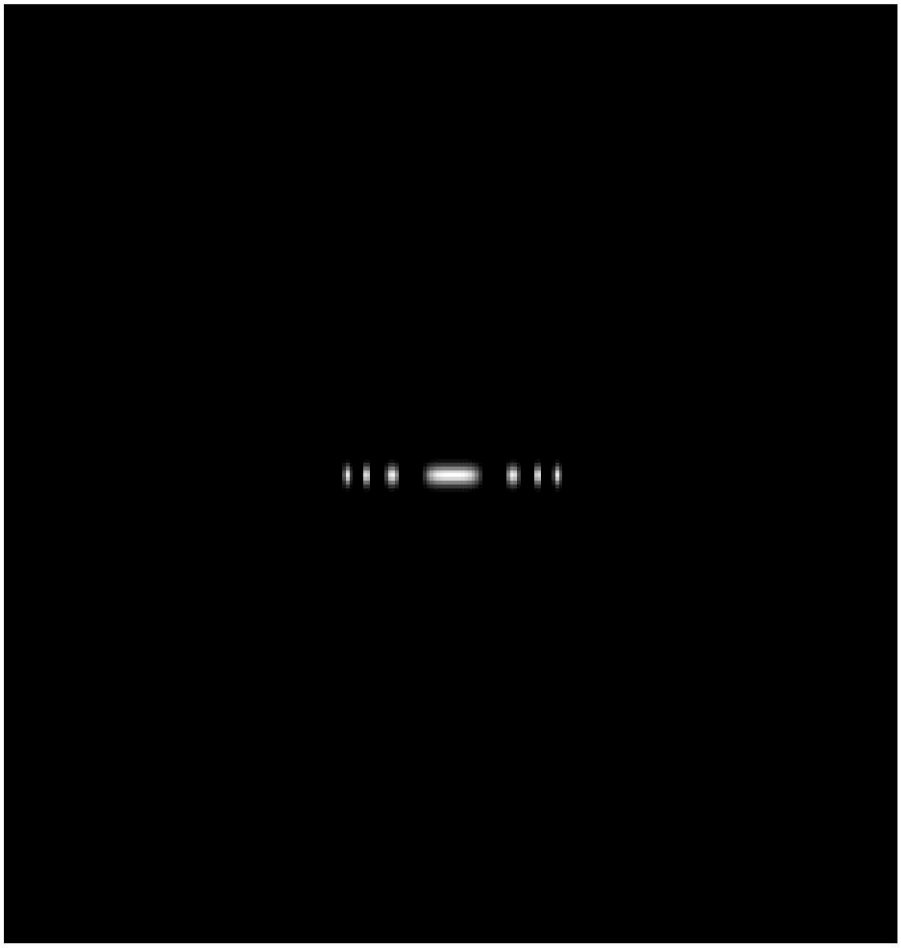

Figure 8 – Wide Gaussian chirp scanning beam

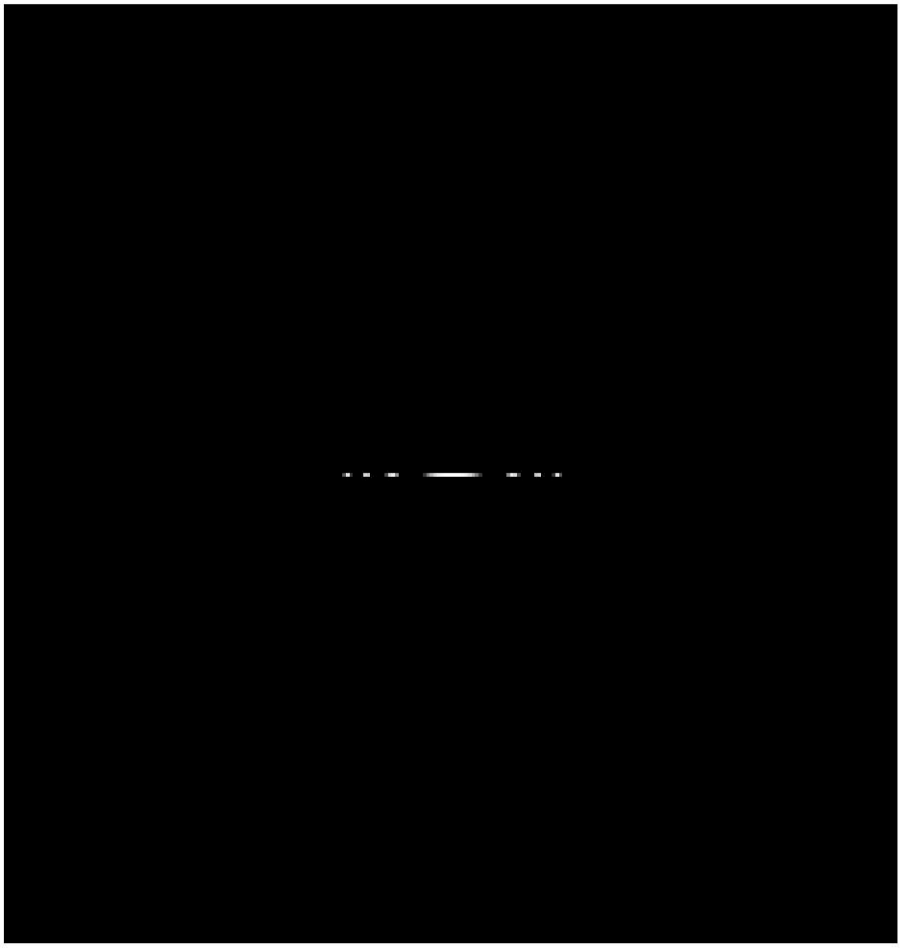

Figure 9 - Narrow Gaussian chirp scanning beam

The sine and cosine holograms obtained using the wide Gaussian Beam are depicted in Figures 10 and 11 respectively.

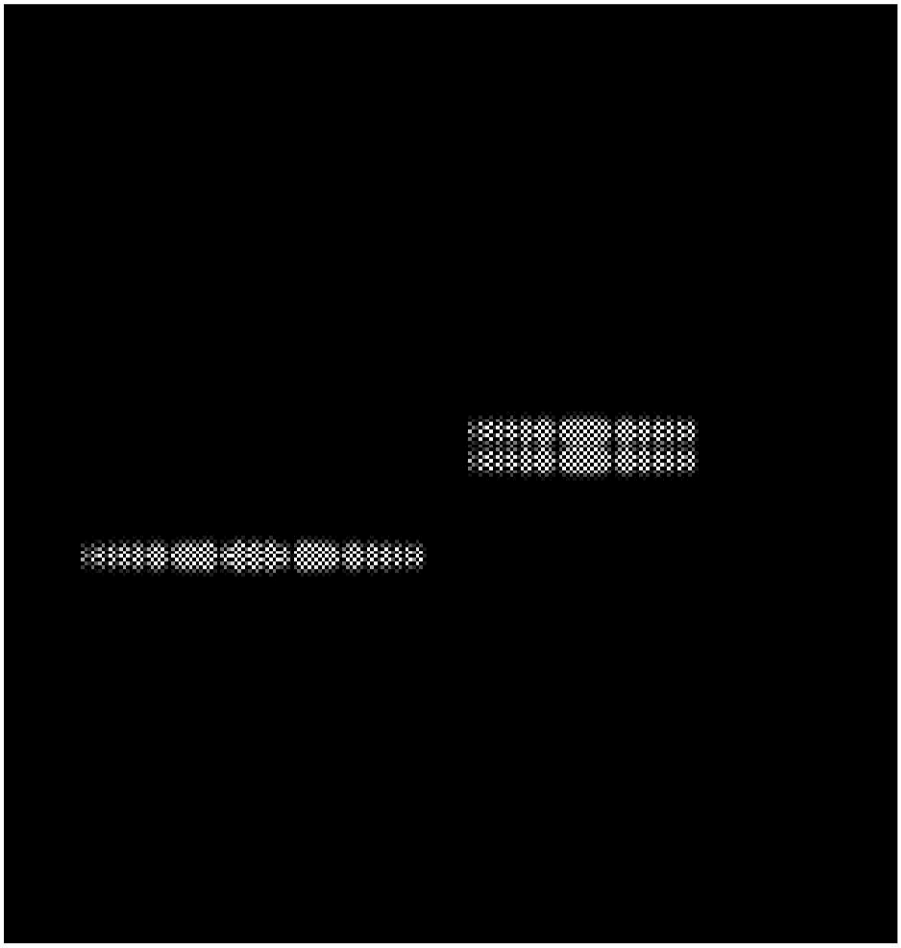

Figure 10 – Sine hologram generated with wide Gaussian beam

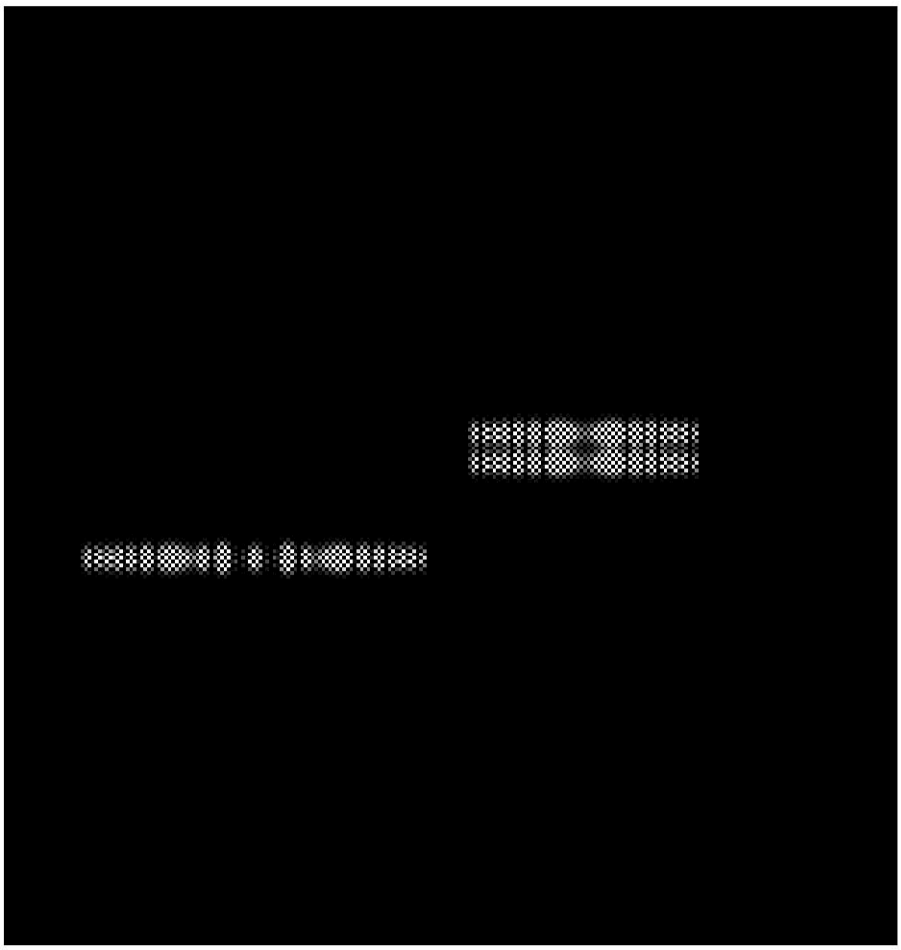

Figure 11 – Cosine hologram generated with wide Gaussian beam

Subsequently, the narrow Gaussian beam was used and the sine and cosine holograms obtained are shown in Figures 12 and 13, respectively.

Figure 12 – Sine hologram generated wide Gaussian beam

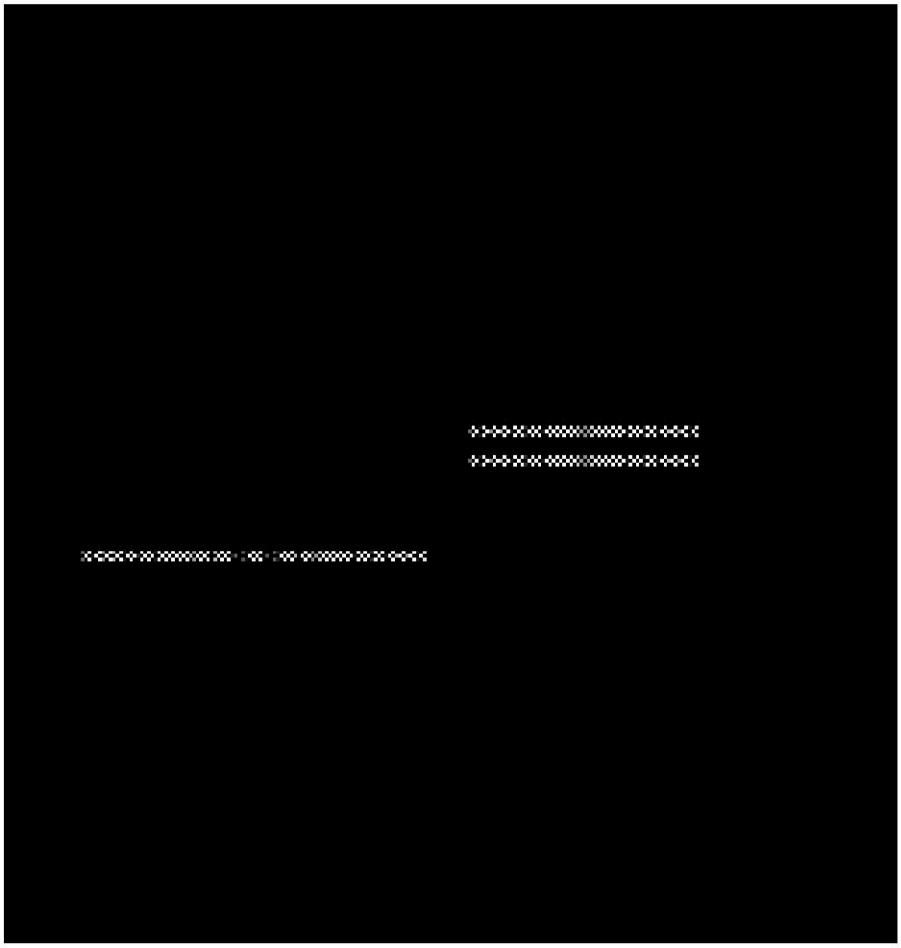

Figure 13 – Cosine hologram generated wide Gaussian beam

The optical reconstruction was simulated digitally. This is done by convolving digitally the complex HPO-hologram with the free space impulse response. This result is depicted in Figures 14 and 15 showing that the dots are holographically focused along the x-direction. However, along the y-direction, the light spreads. The simulations that aim to compensate for this vertical spreading are discussed in Section 3.2.

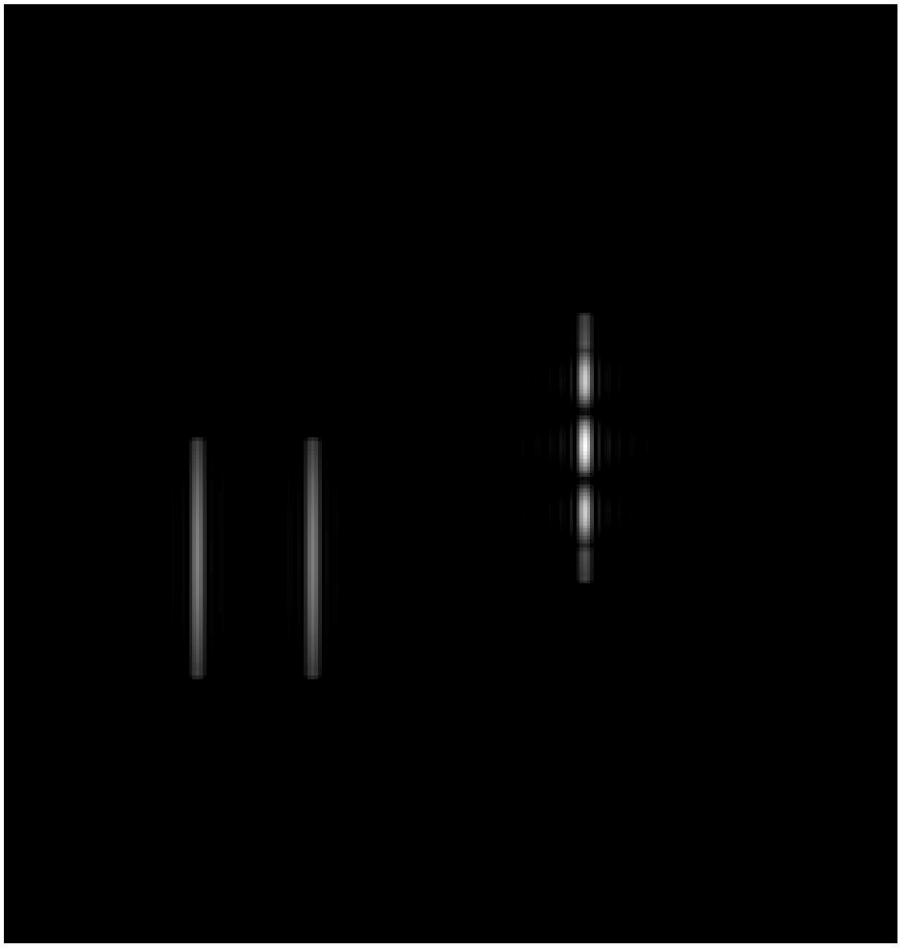

Figure 14 – Reconstructed image where the scanning was done using narrow Gaussian beam

In Figures 14 and 15, two scenarios involving re-constructing holograms that were scanned using narrow and wide Gaussian beam widths were explored. The reconstruction was implemented using a 2-D FZP. In Figure 14, the hologram was scanned using the narrow Gaussian beam shown in Figure 9. In Figure 15, a scenario where the scanning was done by using the wide Gaussian beam in Figure 8.

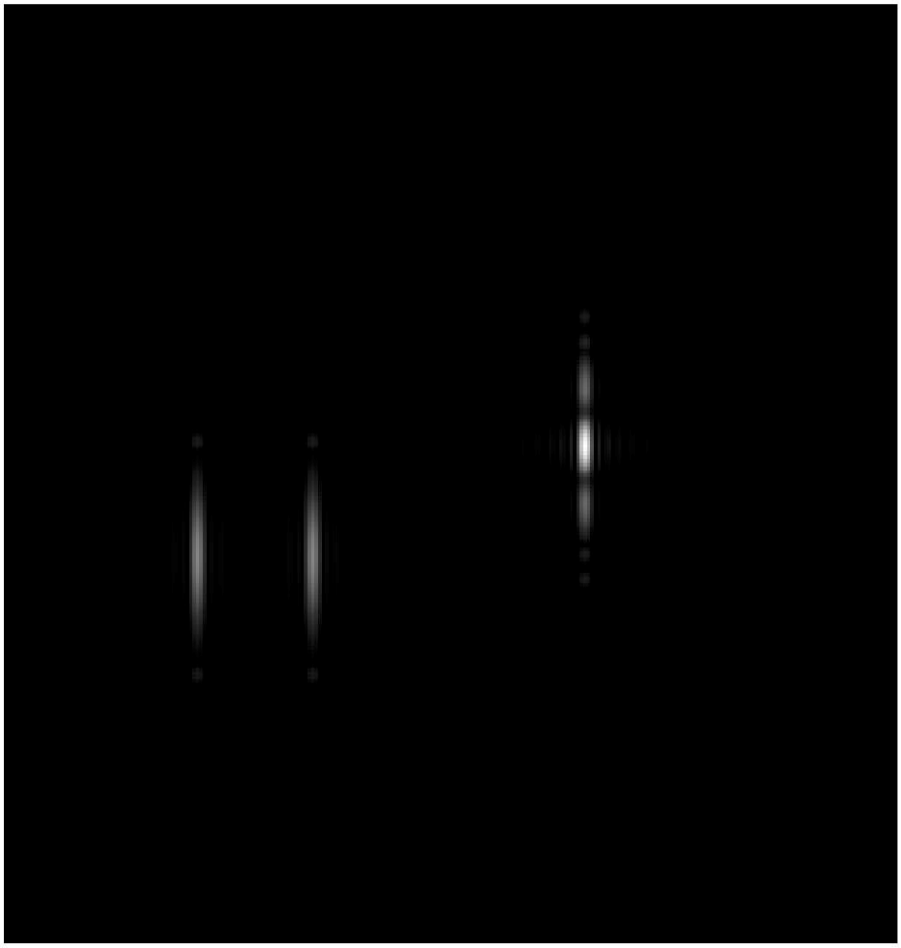

Figure 15 - Reconstructed image where the scanning was done using wide Gaussian beam

The simulations depicted in Figures 14 and 15 demonstrate the effects of the selection of the width of the scanning beam. As shown in Figure 16 an object of size h by h with depth d needs to be scanned by h/ω_y number of holo-lines. The larger this ratio the narrower is the waist of the Gaussian beam. This represents a higher resolution in the vertical direction. [1]. On the other hand, the higher the resolution

the larger is the spread along the y direction after the propagation of depth of the object at distance d. This will result in poorer vertical resolution at the back of the object. Therefore, the waist of the Gaussian beam needs to be optimized for each 3-D object.

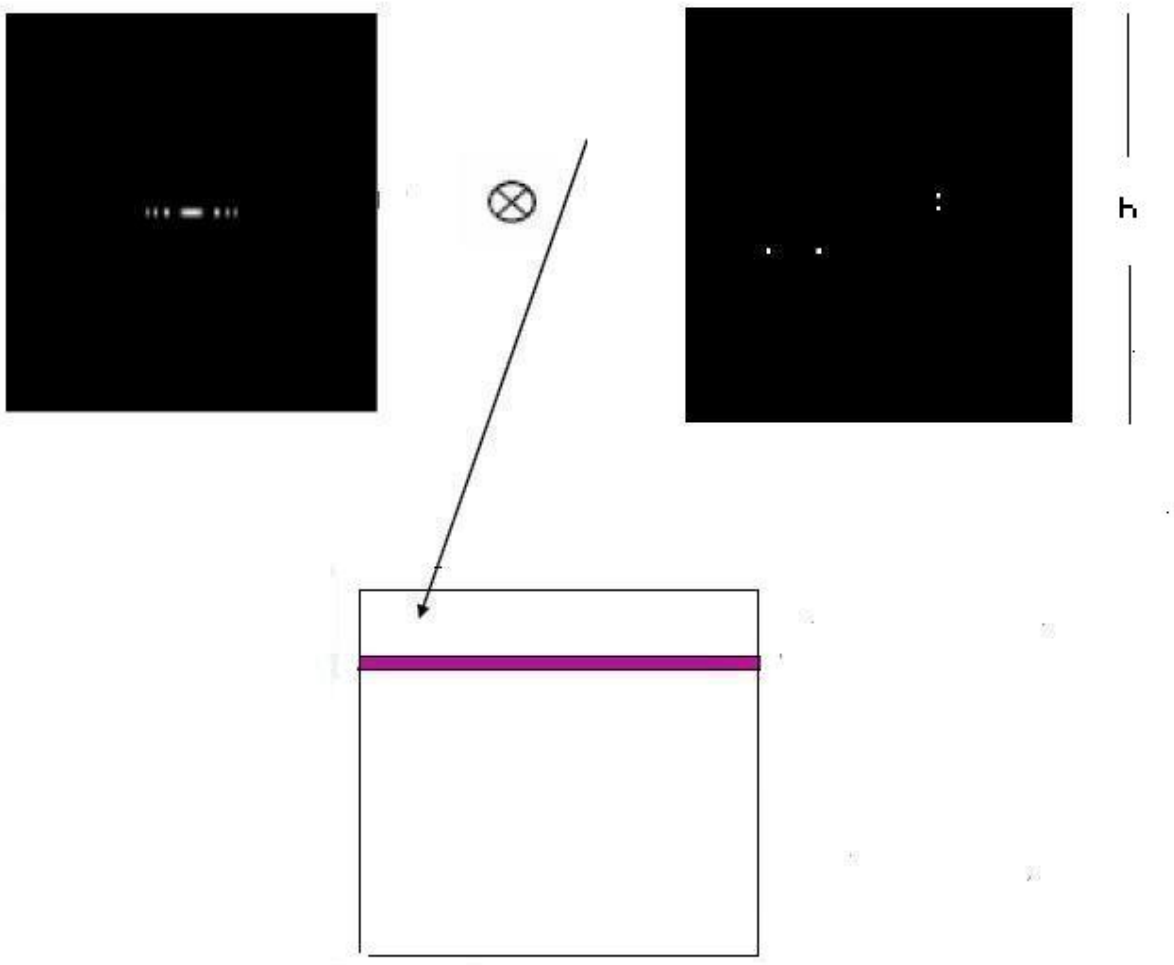

Figure 16 – Horizontal-parallax-only holography concept

3.2 Simulations on optical reconstruction using a cylindrical lens:

HPO-holography yields focused image along the x-direction but results in a spread along the y-direction. This is demonstrated in Figures 14 and 15. An optical reconstruction using a cylindrical lens of focal length $z_0/4$ would compensate for the vertical spread, where z_0 is the distance of the object away from the focused spot on the x-y scanning mirror in the holographic recording setup. This scenario of optical reconstruction is illustrated by Figure 17 [1].

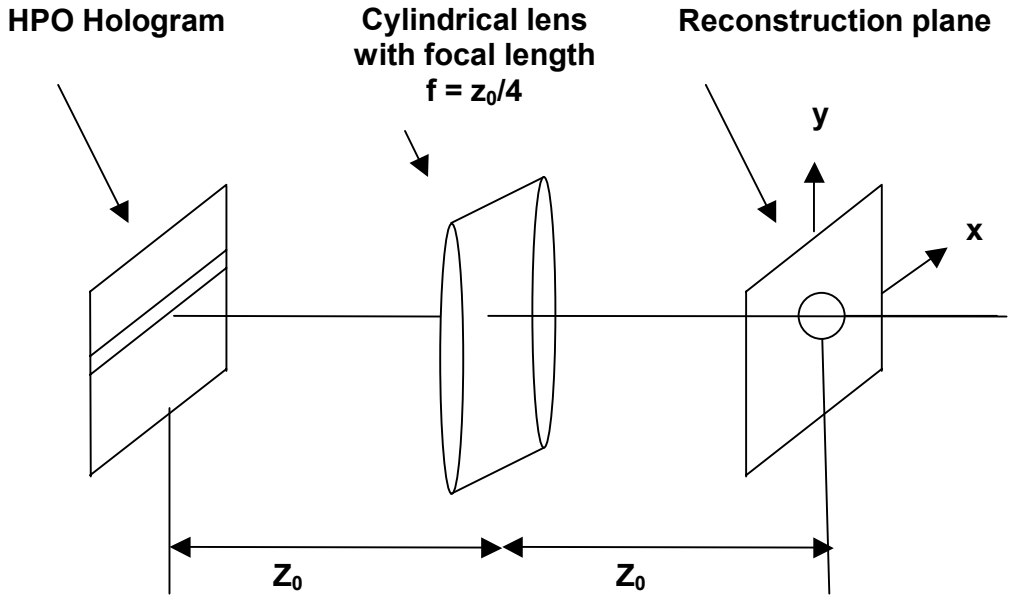

Figure 17 - Optical reconstruction scheme using a cylindrical lens of focal length $z_0/4$ to compensate for the vertical spread

In this case the hologram will provide focusing along the x-direction and the cylindrical lens will provide imaging along the y-direction. This will result in a focused dot on the reconstruction plane with no vertical spread. This is given by

$$\{[H_{c,HPO}(x, y) \otimes h(x, y; z_0/2)] \exp [j(k_0/2f)\, y^2]\} \otimes h(x, y; z_0/2) \qquad \text{(Equation 21)}$$

In Equation (21), the expression $h(x, y; z_0/2)$ represents the propagation from the hologram $H_{c,HPO}(x, y)$ to the cylindrical lens at distance $z_0/2$. $H_{c,HPO}$ is given by Equation (20). The lens action is represented by $\exp[j(k_0/2f)\, y^2]$ with focal length $f = z_0/4$.

In this simulation the complex hologram was constructed using a narrow scan beam in Figure 9. The convolution was implemented by using the relationship defined in Equations (13) and (14). The result of the simulation is depicted in Figure 18.

The optical reconstruction is implemented in the frequency domain as

$$L(x, y) = \mathcal{F}^{-1}\{\mathcal{F}\, [H_{c,HPO}(x, y) \otimes h(x, y; z_0/2)]\} \exp [j(k_0/2f)\, y^2] \qquad \text{(Equation 22)}$$

and

$$\mathcal{F}^{-1}\{\mathcal{F}[L(x, y) \otimes h(x, y; z_0/2)]\}. \qquad \text{(Equation 23)}$$

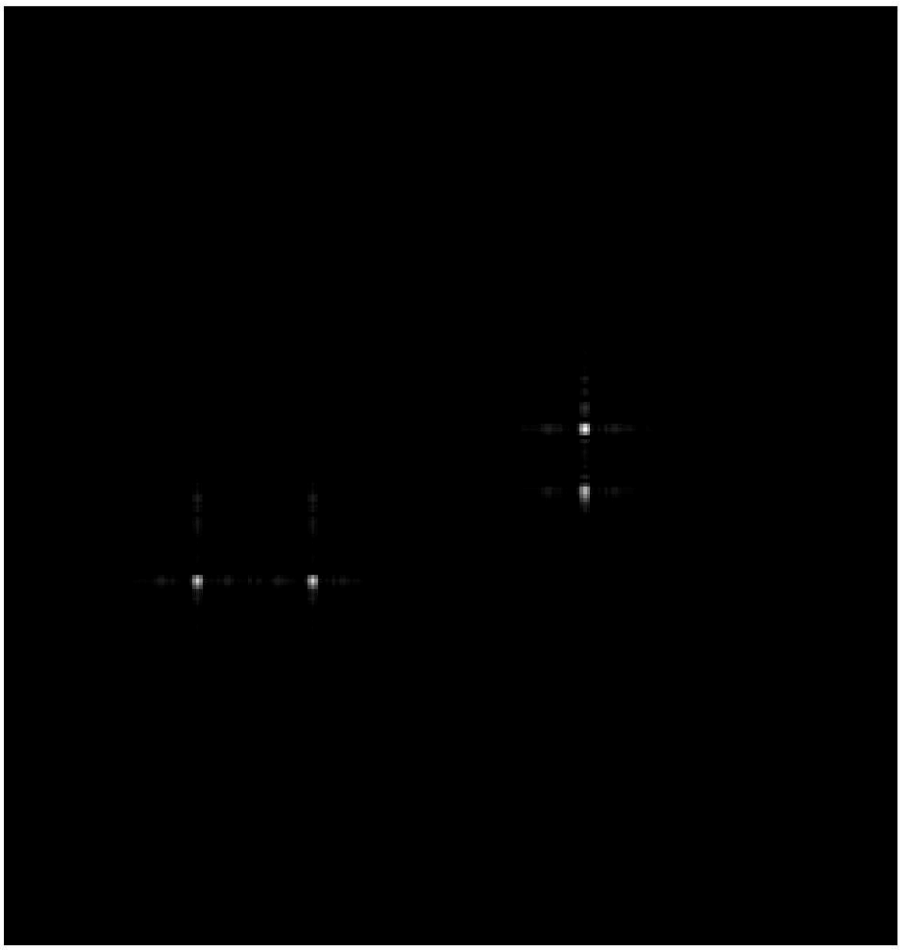

Figure 18 – Optical construction using cylindrical lens cylindrical lens of focal length $z_0/4$ at distance z_0

3.3 Simulations involving 2-planes separated by z_0 along depth:

This program simulation depicts a scenario where the left half and the right half of the image are at a distance z_0 and $2z_0$ away from the scanning beam, and hence the 3D object is described along depth. The simulations were executed by using Gaussian Chirp scanning beams [See Equation (18)] of different widths. As described in Section 3.1, the narrow beam was implemented by setting $\omega_x = 1000\omega_y$ in Equation (15). The Gaussian Chirp beam was allowed to propagate for $2z_0$. These beams are depicted in Figures 19 and 20 respectively. The same input image depicted in Figure 3 was used in this simulation. The sine and cosine holograms obtained are shown in Figures 21 and 22 respectively.

The holograms are constructed at z_0 and $2z_0$ using the Chirp Gaussian beams and 2D Fresnel zone plate shown in Figure 4. The following scenarios were considered:

Scenario 1 - Reconstruction with Gaussian Chirp scanning beam at z_0: This simulation is shown in Figure 23. Since the left hand side of the image was scanned with the Chirp Gaussian beam at z_0, the dots in the left hand side are in focus. However, the dots scanned at $2z_0$ in the right plane are blurred. There is no vertical spread due to reconstruction with a Gaussian Chirp beam

Scenario 2 - Reconstruction with 2D FZP at z_0. This scenario is depicted in Figure 24. Reconstruction with 2D FZP resulted in spread in the y direction in both planes. Similarly to Scenario 1 the left hand side of the image that was scanned with the Chirp Gaussian beam at z_0 was in focus along x. The dots on the right hand side are blurred.

Scenario 3 - Reconstruction with diffracted Gaussian Chirp scanning beam at $2z_0$: This scenario is shown in Figure 25. Since the right hand side of the image was reconstructed with the diffracted Gaussian beam at $2z_0$, the dots in the right hand side are in focus. However, the dots scanned at z_0 in the left plane are blurred. As in Scenario 1, there is no vertical spread due to reconstruction with the Gaussian chirp beam.

Scenario 4 - Reconstruction with FZP at $2z_0$: This scenario is depicted in Figure 26. Similar to Scenario 2, reconstruction with 2D FZP resulted in spread in the y direction in both planes. The right hand side of the image that was scanned with the Gaussian Chirp beam at $2z_0$ was in focus. The dots on the left hand side that were scanned at z_0 are blurred.

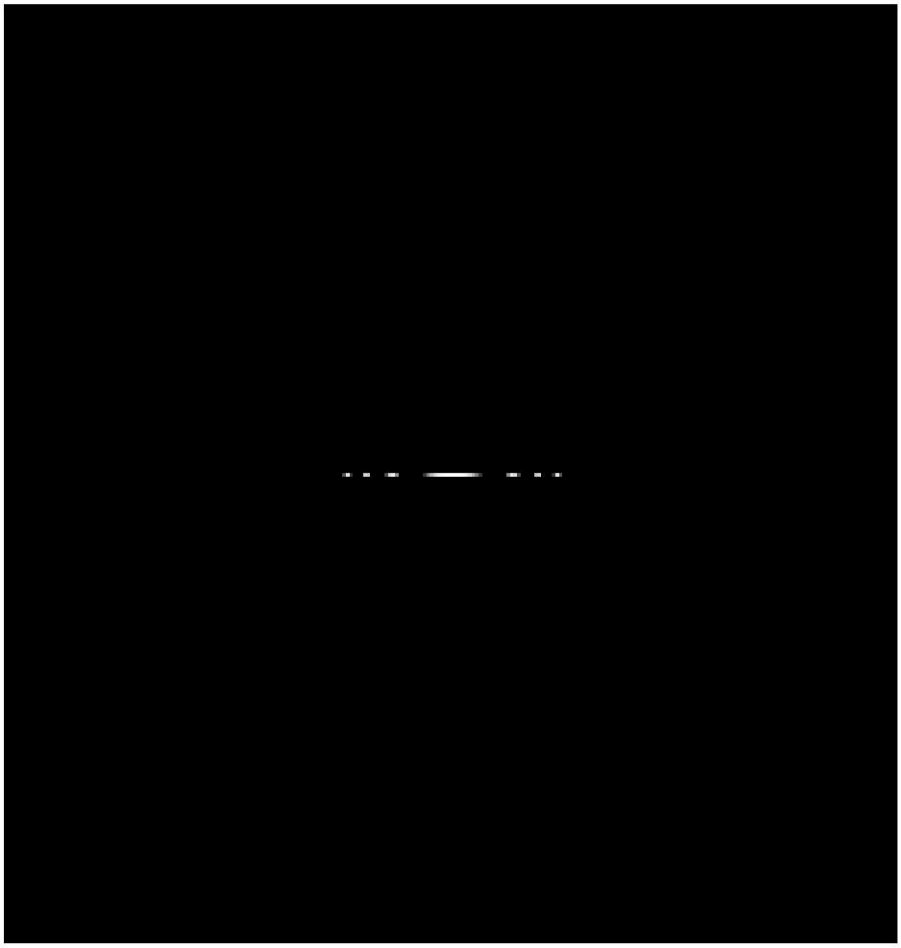

Figure 19 – Gaussian chirp beam (z_0) that was for scanning the left hand plane

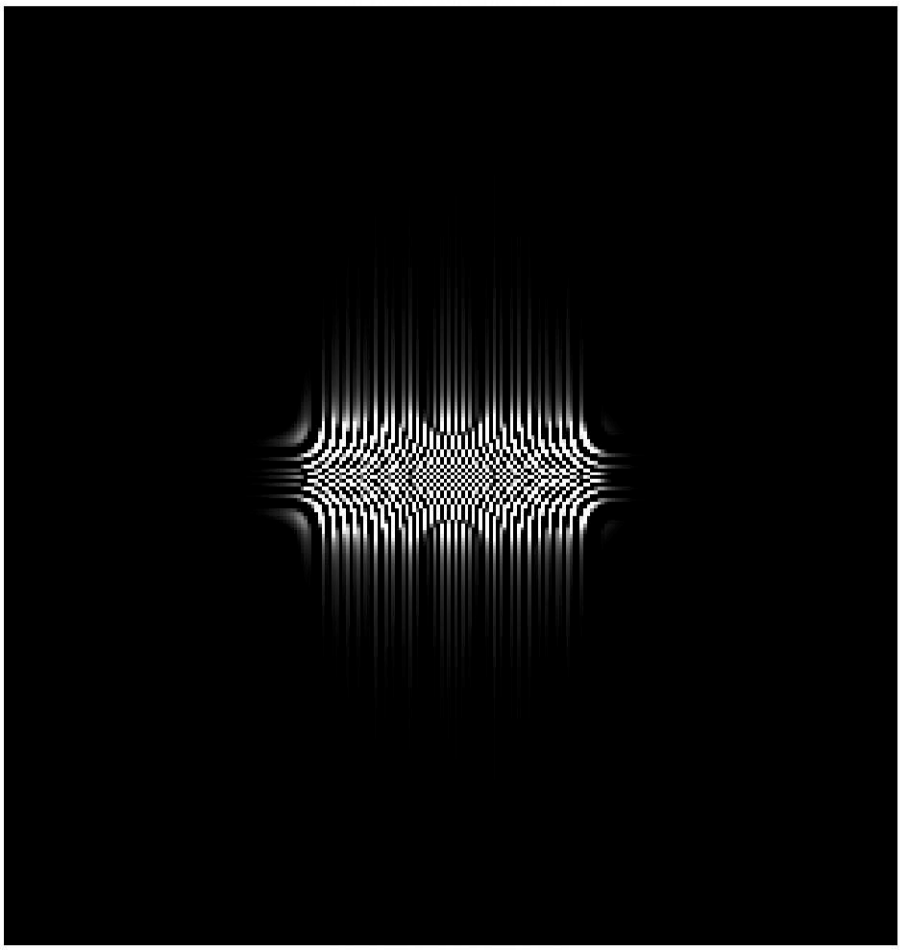

Figure 20 - Diffracted Gaussian chirp beam ($2z_0$) that was for scanning the right hand plane

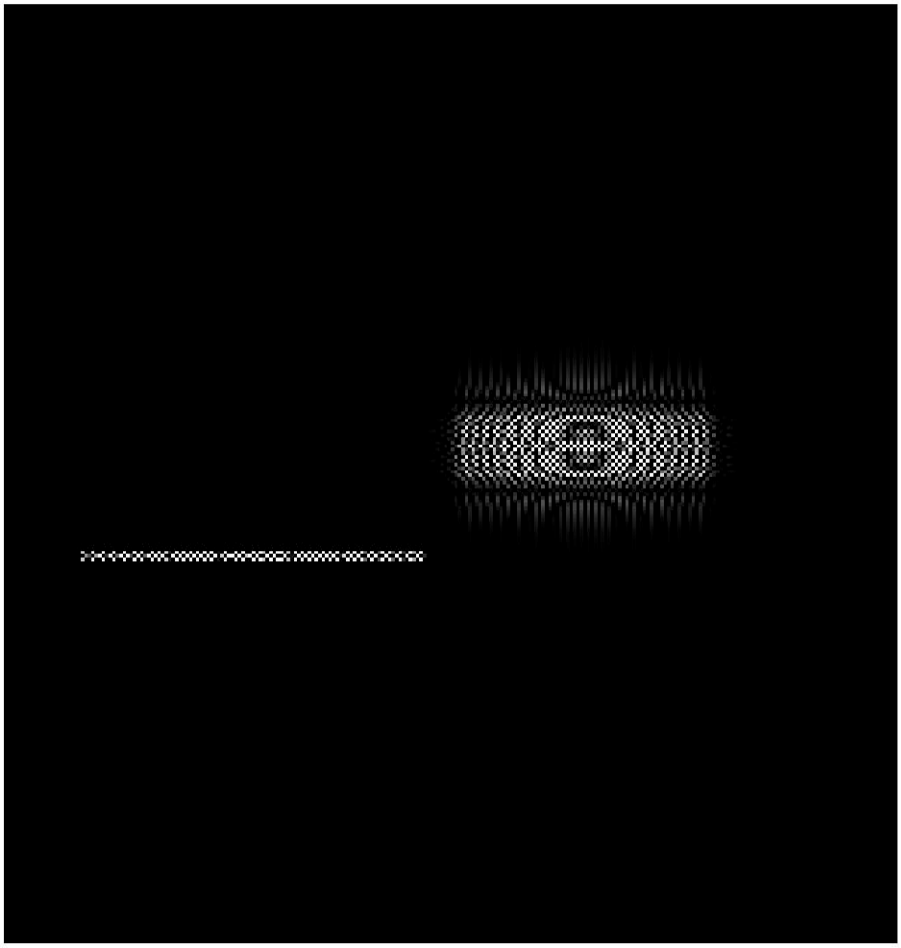

Figure 21 – Sine hologram

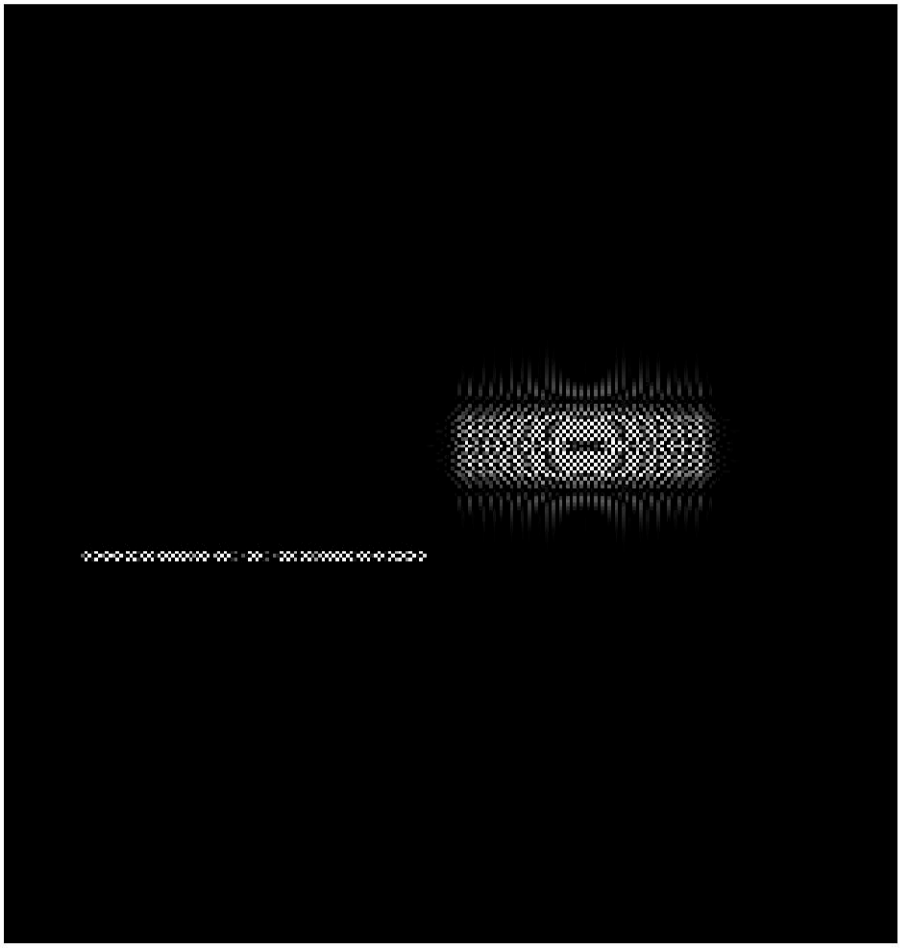

Figure 22 – Cosine hologram

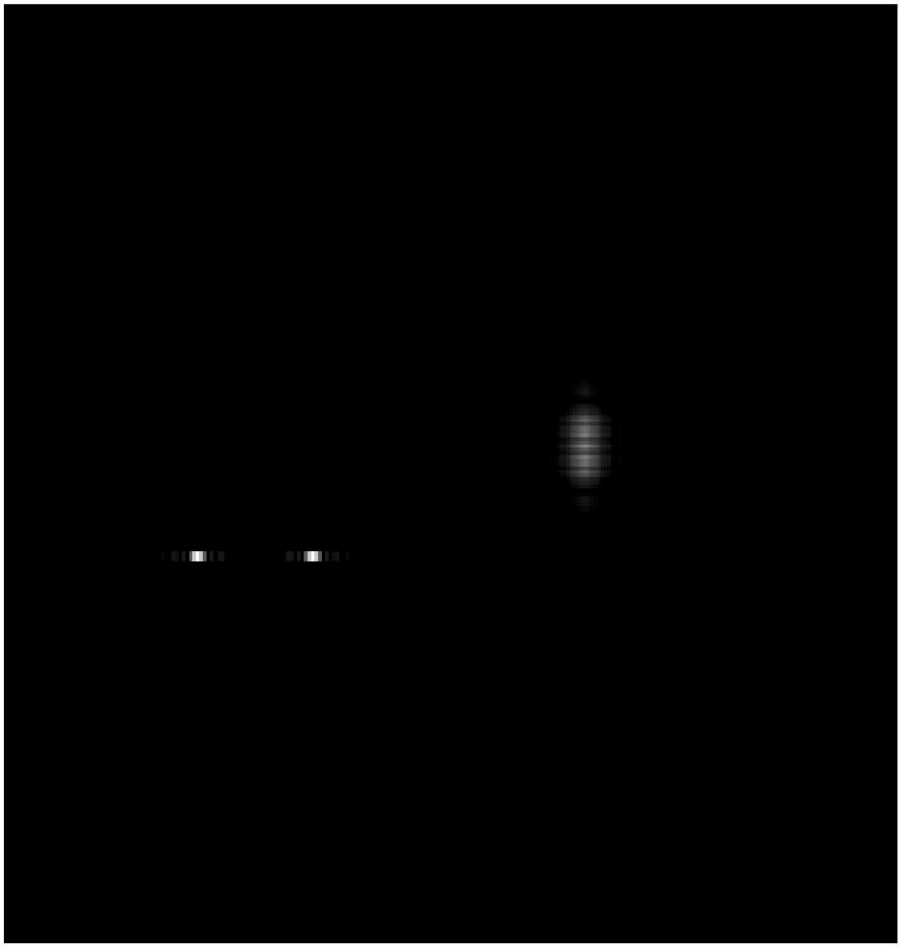

Figure 23 – Reconstruction with narrow Gaussian Chirp beam at z_0

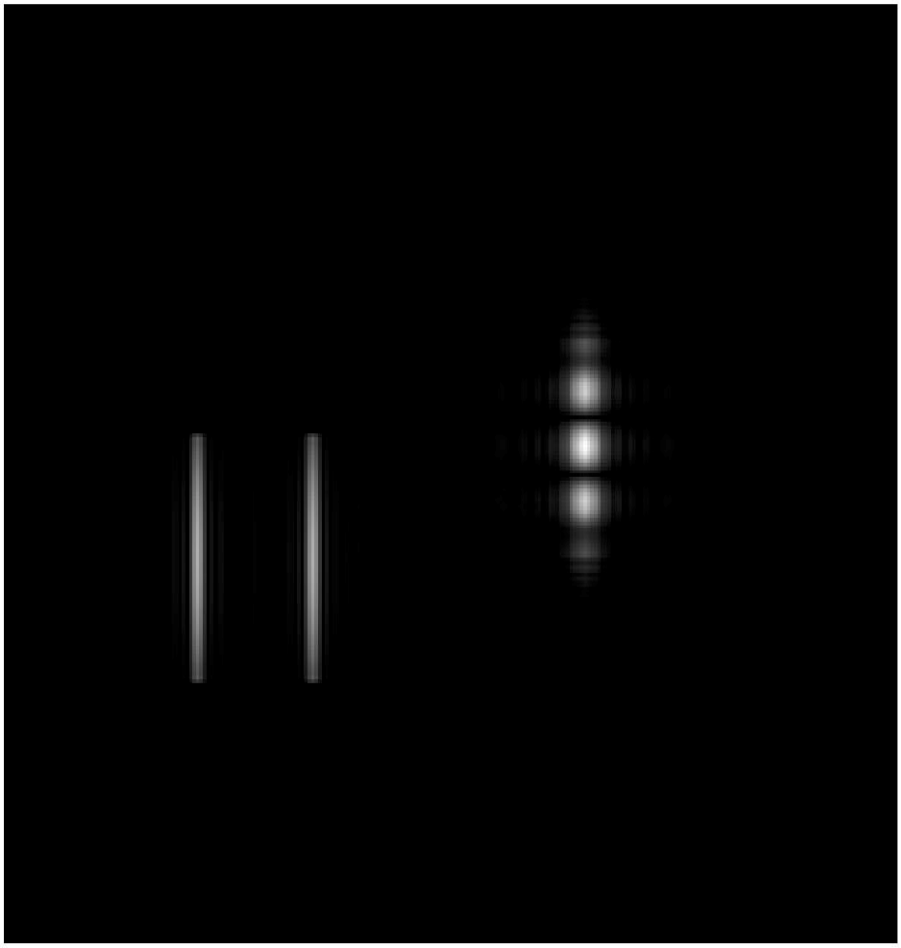

Figure 24 – Reconstruction with 2-D Fresnel Zone Plate at z_0

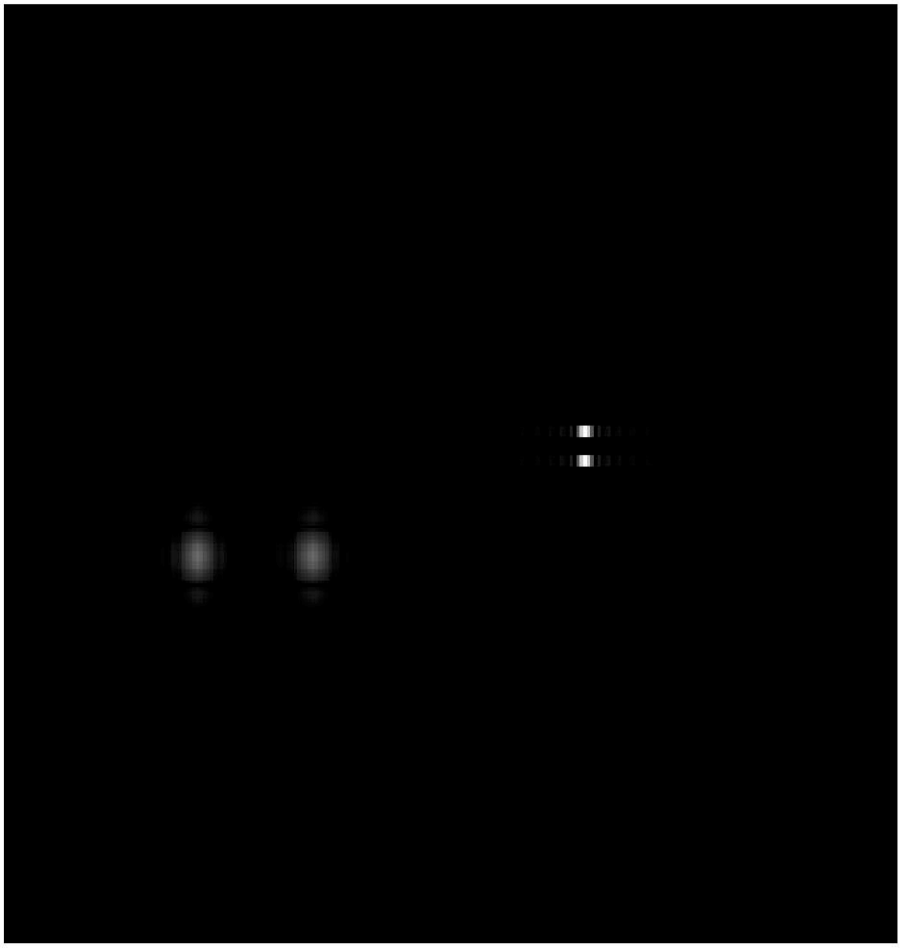

Figure 25 – Reconstruction with diffracted Gaussian Chirp beam at $2z_0$

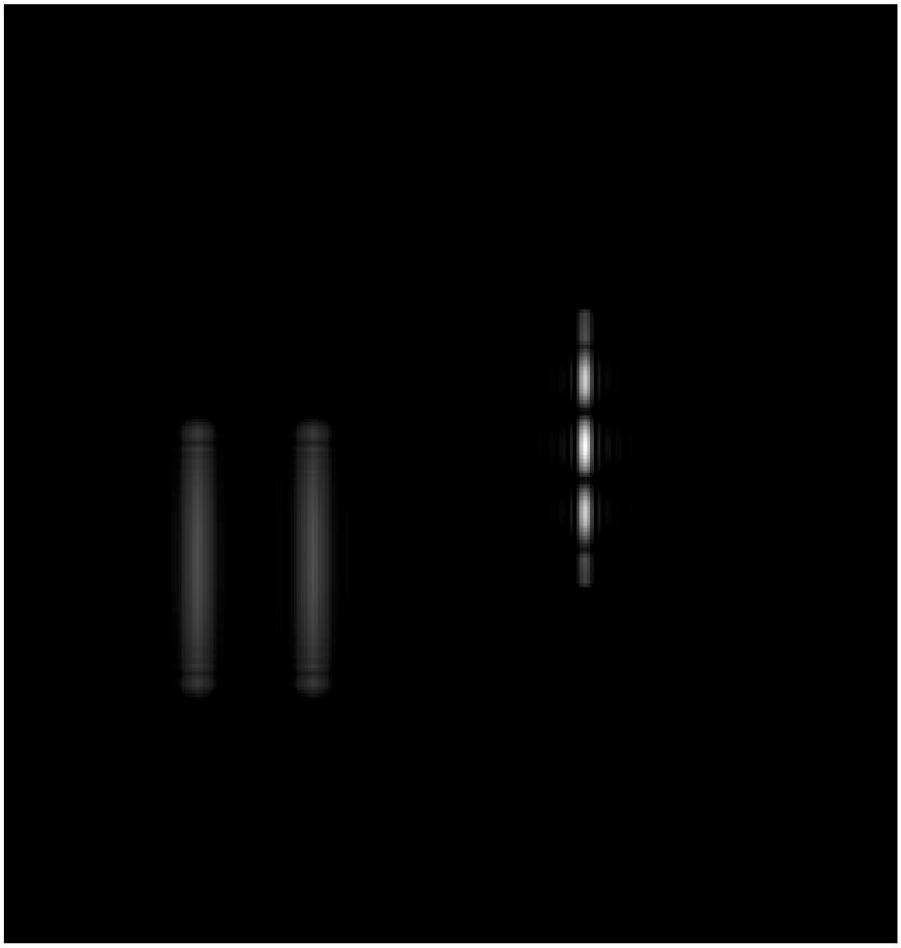

Figure 26 – Reconstruction with 2-D Fresnel Zone Plate at $2z_0$

Chapter 4: Conclusion and Future Work

The purpose of this thesis has been the investigation of the recoding of horizontal-parallax-only holographic information and simulations in optical holographic reconstruction. The investigation has been primarily based on computer simulations. The input images and the holograms have been digitally generated and the reconstruction has been done digitally using MATLAB.

Although many ideas of HPO-holography have been proposed and studied, to the best of my knowledge, this is the first proposed electronic technique to acquire HPO-holographic information [1]. The simulations demonstrate that holographic information reduction techniques also help to alleviate the problems associated with the restricted field of view upon holographic reconstruction for 3-D display. The simulations show that and horizontal-parallax-only holography is an excellent way to reduce holographic and an optical reconstruction scheme could be used to record holograms. This could be performed by 2-D active optical scanning of a 1-D time dependent FZP onto the 3-D object to generate a complex HPO-OSH. The 1-D scanning zone plate could be implemented by masking the 2-D zone plate with a horizontal slit. In this thesis, the 1- D scanning was implemented using a narrow Gaussian Chirp function. This idea is demonstrated by the simulations in this thesis. Accordingly, the holographic recording could be achieved by the proposed reconstruction system.

In this scenario, an optical recording (shown in Figure 27) using a lens will basically image the Gaussian chirp beam on Plane 1 for the 3-D object to be x-y scanned. This will result in a focused dot on the reconstruction plane with no vertical

spread. In this scenario, the electronic detection could be implemented as in conventional OSH.

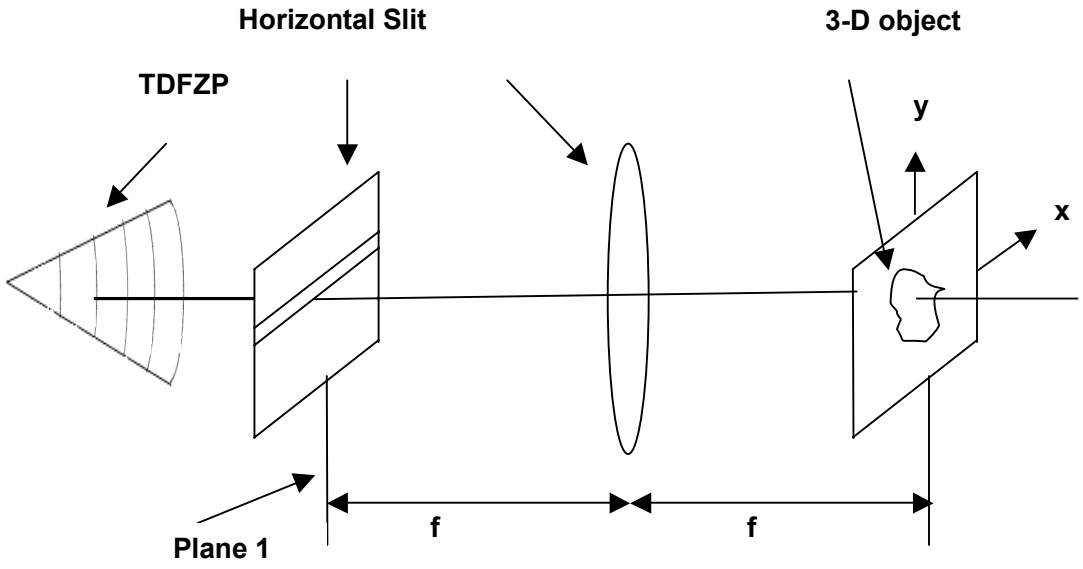

Figure 27 – Proposed setup for optical recording using a lens of focal length f

HPO-OSH helps reduce the information content of holograms to facilitate the transmission. Presently, there are at least two 3-D display systems for HPO-OSH electronic holograms [2, 17]. The proposed system in Figure 27 would render it feasible to acquire HPO-OSH holographic information from real objects. Combining the two systems will result in realizing a 3-D holographic television network.

The simulations in this thesis demonstrate the effects of the selection of the width of the scanning beam. The narrower the waist of the Gaussian beam, the higher the resolution in the vertical direction [2]. On the other hand, the higher the resolution the larger the spread along the y direction upon reconstruction. Therefore, the waist of the Gaussian beam needs to be optimized for each 3-D object.

The simulations in this thesis pave the way to digitally and optically explore the implementation of this setup. Since there is a 3-D display system for HPO-electronic holograms already, and with the present proposed system, one could acquire HPO-electronic holographic information from real objects. Thus, we envision the incorporation of the two systems to finally achieve the goal of 3-D holographic television system in the near future [1]. As a follow up to this simulation, we suggest future work include actual experimentation to verify the ideas presented in this thesis.

References

[1] Poon, T.-C., Akin, T., Indebetouw, G and Kim, T. (2005). Horizontal-parallax-only electronic holography, Optics Express, 13, 2427-2432.

[2] Lucente, M. (1992). Optimization of Hologram Computation for Real-Time Display, SPIE Proceedings, 1136, 1667-1704.

[3] Poon, T.-C. (2002). Three-dimensional television using optical scanning holography, Journal of Information Display, 3, 12-16.

[4] Poon, T.-C. (2004). Recent progress in optical scanning holography, Journal of Holography and Speckle, March, 6-25.

[5] Poon, T.-C. and Korpel, A. (1979). Optical transfer function of an acousto-optic heterodyning image processor, Optics Letter, 4, 317-319.

[6] Poon, T.-C. (1985). Scanning holography and two-dimensional image processing by acousto-optic two pupil synthesis, Journal of the Optical Society of America, 2, 521-527.

[7] Poon, T.-C. and Kim, T. (1999). Optical image recognition of three-dimensional objects, Applied Optics 38(2), 370-381.

[8] Poon, T.-C., Wu, MH., Shinoda, K. and Suzuki Y. (1996). Optical scanning holography, Proceedings of the IEEE, 84(5), 753-764.

[9] Indebetouw, G. and Poon, T.-C., (1986), Parallel synthesis of bi-polar point spread functions in a scanning heterodyne optical system, Optica-Acta, 23, 827- 834.

[10] Kim, T. (1997). Optical scanning holography for 3-D imaging of fluorescent object in turbid media, Master's Thesis, Virginia Tech, Blacksburg, VA.

[11] Schilling, BW. (1997). Three-dimensional fluorescence microscopy by optical scanning holography, Doctoral dissertation, Virginia Tech, Blacksburg, VA.

[12] Poon, T.-C. and Indebetouw, G. (2003). Three-Dimensional Point Spread Functions of an Optical Heterodyne Scanning Image Processor, Applied Optics, 42, 1485-1492.

[13] Poon, T.-C. and Banerjee, BB. (2001). Contemporary topics in optical image processing, In Poon, T.-C. and Banerjee, PP., Contemporary Optical Image Processing with Matlab, Oxford, UK: Elsevier.

[14] Poon, T.-C., "T.-C. Poon, Kim, T. and Doh, K. (2003). Optical Scanning Cryptography for Secure Wireless Transmission, Applied Optics, 42, 6496-6503.

[15] Poon, T.-C. and Banerjee, BB. (1991). Principles of applied optics, Boston: Irwin.

[16] Poon, T.-C. and Kim, T., Indebetouw, G., Wu, MH., Shinoda, K. and Suzuki, Y. (2000). Twin-image elimination experiments for three-dimensional images in optical scanning holography, Optics Letters, 25, 215-217.

[17] Yoshikawa, H. and Sasaki, K. (1993). Information reduction by limited resolution for electro-holographic display, SPIE Proceedings of Practical Holography VII, 1914, 1914-1930.